

**Cyclotron resonance energies at a low X-ray luminosity:
A0535+262 observed with *Suzaku***

Y. Terada¹, T. Mihara¹, M. Nakajima¹, M. Suzuki¹, N. Isobe¹, K. Makishima^{1,2},
H. Takahashi², T. Enoto², M. Kokubun², T. Kitaguchi², S. Naik³, T. Dotani³, F. Nagase³,
T. Tanaka³, S. Watanabe³, S. Kitamoto⁴, K. Sudoh⁴, A. Yoshida⁵, Y. Nakagawa⁵,
S. Sugita⁵, T. Kohmura⁶, T. Kotani⁷, D. Yonetoku⁸, L. Angelini⁹, J. Cottam⁹,
K. Mukai⁹, R. Kelley⁹, Y. Soong⁹, M. Bautz¹⁰, S. Kissel¹⁰, and J. Doty¹¹

terada@riken.jp

ABSTRACT

The binary X-ray pulsar A0535+262 was observed with the *Suzaku* X-ray observatory, on 2005 September 14 for a net exposure of 22 ksec. The source was in a declining phase of a minor outburst, exhibiting 3–50 keV luminosity of $\sim 3.7 \times 10^{35}$ ergs s⁻¹ at an assumed distance of 2 kpc. In spite of the very low source intensity (about 30 mCrab at 20 keV), its electron cyclotron resonance was

¹Cosmic Radiation Laboratory, Institute of Physical and Chemical Research, Wako, Saitama, Japan 351-0198

²Department of Physics, University of Tokyo, 7-3-1 Hongo, Bunkyo-ku, Tokyo, Japan 113-0033

³Institute of Space and Astronautical Science, JAXA, 3-1-1 Yoshinodai, Sagamihara, Kanagawa, Japan 229-8510

⁴Department of Physics, Rikkyo University, 3-34-1 Nishi-Ikebukuro, Toshima-ku, Tokyo, Japan 171-8501

⁵Department of Physics & Math., Aoyama Gakuin University, Sagamihara, Kanagawa, Japan 229-8558

⁶Department of Physics, Kogakuin University, 2665-1 Nakano, Hachi-oji, Tokyo, Japan 192-0015

⁷Department of Physics, Tokyo Tech, 2-12-1 O-okayama, Meguro-ku, Tokyo, Japan 152-8551

⁸Department of Physics, Kanazawa University, Kadoma, Kanazawa, Ishikawa, Japan 920-1192

⁹Exploration of the Universe Division, Code 660, NASA/GSFC, Greenbelt, MD 20771, USA

¹⁰Kavli Institute for Astrophysics and Space Research, Massachusetts Institute of Technology, 77 Massachusetts Avenue, Cambridge, MA 02139

¹¹Noqsi Aerospace, Ltd., 2822 South Nova Road, Pine, Colorado, 80470, USA

detected clearly with the *Suzaku* Hard X-ray Detector, in absorption at about 45 keV. The resonance energy is found to be essentially the same as those measured when the source is almost two orders of magnitude more luminous. These results are compared with the luminosity-dependent changes in the cyclotron resonance energy, observed from 4U 0115+63 and X0331+53.

Subject headings: magnetic fields — pulsars: individual (A0535+26) — stars:neutron — X-rays: binaries

1. Introduction

Binary pulsars are considered to have strong surface magnetic fields in the range of 10^{12-13} Gauss. Their field strengths can be directly measured through energies of cyclotron resonance scattering features (CRSFs), which often appear in their X-ray spectra (e.g. Mihara 1995; Makishima et al. 1999). Neglecting the gravitational redshift, the magnetic field strength B is then calculated from the resonance energy E_a through a relation of E_a (keV) = $11.6 B / (10^{12} \text{ Gauss})$.

Since the magnetic field must be intrinsic to a pulsar, the CRSF energy was believed to be constant in each object. However, a $\sim 35\%$ change in the cyclotron energy was unexpectedly observed with *Ginga* from the recurrent transient pulsar 4U 0115+63, between its 1990 and 1991 outbursts (Mihara 1995; Mihara et al. 1998, 2004). The change is considered to reflect luminosity-dependent variations in the accretion-column height by several hundred meters, assuming a dipolar field configuration (Mihara et al. 2004). The effect was studied in further detail by Nakajima et al. (2006), using the *RXTE* data of 4U 0115+63 which continuously covered another outburst in 1999. At that time, the CRSF energy was confirmed to increase from ~ 11 keV to ~ 16 keV, as the 3–50 keV source luminosity (at an assumed distance of 7 kpc; Negueruela & Okazaki 2001) decreased across a relatively narrow range of $(2 - 4) \times 10^{37} \text{ ergs s}^{-1}$.

From another source, X0331+53 (V0332+53), a similar effect was detected with *INTEGRAL* (Mowlavi et al. 2006) and *RXTE* (Nakajima 2006b). The change in the CRSF energy, however, started in this case at a higher luminosity of $2 \times 10^{38} \text{ ergs s}^{-1}$, assuming this object to have a distance of 7 kpc as well (Negueruela et al. 1999). Thus, the luminosity-dependent change in the CRSF energy is emerging as a new intriguing issue, of which a unified view is yet to be constructed.

This *Letter* deals with A0535+262, yet another recurrent transient with a 103 sec pulsation period and a 111 day orbital period, located at a distance of 2.0 kpc (Steele et al.

1998). Its CRSFs were discovered at 50 and 100 keV by the TTM and HEXE instruments onboard *Mir-KVANT* in a 1989 outburst (Kendziorra et al. 1994), and the 2nd harmonic was later reconfirmed at 110 keV with the *CGRO* OSSE (Grove et al. 1995). Since this pulsar has the *highest* measured CRSF energy, it is of particular interest to compare this object with 4U 0115+53, which has the *lowest* known CRSF energy. However, the previous CRSF measurements from A0535+262 were all limited to very luminous states. Here, we report on a successful detection of the CRSF from this source by *Suzaku*, made for the first time at a very low luminosity of $\sim 4 \times 10^{35}$ ergs s⁻¹ (Inoue et al. 2005).

2. Observations and Data Reduction

According to *RXTE* ASM monitoring, A0535+262 entered outburst twice in 2005. On the first occasion, the 2–10 keV intensity reached a peak of 1.3 Crab ($\sim 1 \times 10^{38}$ ergs s⁻¹ in luminosity) on June 6. The second outburst, an order of magnitude smaller, took place about one binary orbital period later, reaching the peak on September 1. On 2005 August 28 when the 2–100 keV luminosity was 1.2×10^{37} ergs s⁻¹, the CRSF was detected at 48.5 ± 0.7 keV with the *RXTE* (Wilson & Finger 2005). The same feature was confirmed with the *INTEGRAL* SPI at 47 ± 2 keV on August 31 (Kretschmar et al. 2005). These measurements refer to Gaussian modeling of the observed absorption features.

The fifth Japanese X-ray satellite, *Suzaku*, was launched on 2005 July 10. It carries onboard the X-ray Imaging Spectrometer (XIS) operating in 0.2–12 keV (Matsumoto et al. 2005), and the Hard X-ray Detector (HXD; Kawaharada et al. 2004) which covers 10–70 keV with PIN diodes and 40–600 keV with GSO scintillators.

We observed A0535+262 with *Suzaku* from 13:40 UT on 2005 September 14 to 01:00 UT the next day, when the source was in the declining phase of the second outburst. The observation was carried out at “XIS nominal” pointing position, for a net exposure of 22.3 ksec with the XIS and 21.7 ksec with the HXD. The XIS was operated in the normal mode with “1/8 window” option, which gives a time resolution of 1 sec, whereas the HXD was in the nominal mode.

The source was detected with the XIS at an intensity of 10 cts s⁻¹ per sensor. In the XIS analysis, we excluded all the telemetry saturated data portions, and data taken in “low” rate mode. We further removed those time intervals when the source elevation above the earth’s limb was below 5° or the spacecraft was in the South Atlantic Anomaly (SAA). We then accumulated nominal-grade events within 6 mm (4'.3) of the image centroid. The XIS background spectra were taken from a blank sky observation towards the North Ecliptic Pole

region, conducted for 95 ksec on 2005 September 2–4.

The HXD data were screened using the same criteria as for the XIS. In addition, we discarded data taken up to 436 s after leaving the SAA, and those acquired during time intervals where the geomagnetic cutoff rigidity was lower than 8 GeV/c. After this filtering, the final HXD event list was obtained only using events that survived the standard anti-coincidence function of the HXD.

The non X-ray background of the PIN diodes was synthesized by appropriately combining night-earth data sets acquired under different conditions (Kokubun et al. 2006). The GSO background was derived from a source-free observation performed on 2005 September 13, namely, immediately before the pointing onto A0535+26. The background GSO events were accumulated over identical orbital phases of *Suzaku* as the on-source data integration, resulting in an exposure of 19 ksec. Though rather short, this particular dataset is considered best in minimizing systematic errors associated with the GSO background estimation. After subtracting these backgrounds, the source was detected significantly at an intensity of 1.4 cts s⁻¹ (10–70 keV) with PIN, and 0.4 cts s⁻¹ (40–200 keV) with GSO.

3. Results

Figure 1 shows the background-subtracted XIS and HXD spectra of A0535+262, averaged over the whole observation. The 0.5 – 100 keV X-ray flux is measured as 9.4×10^{-10} ergs s⁻¹ cm⁻², yielding an X-ray luminosity of 4.5×10^{35} ergs s⁻¹ in the same band. In Figure 1, we also show typical PIN and GSO non X-ray backgrounds, and uncertainties in their reproducibility which are $\sim \pm 5\%$ for PIN and $\sim \pm 2\%$ for GSO; both these estimates are specific to the present observing conditions, and are based on the *current* level of instrumental calibration. Thus, the statistical errors are dominant in the PIN spectrum, whereas the statistical and systematic errors are comparable in the GSO data particularly above 100 keV. The contribution of the cosmic X-ray background is only $\sim 3\%$ of the signal, and hence negligible, but it was subtracted in deriving the PIN spectrum in Figure 1.

The source pulsations were detected at a barycentric period of 103.375 ± 0.09 sec, over the full XIS band and at least up to 100 keV with the HXD. As shown in Figure 1 inset, the pulse profiles are similar to those previously obtained with *Ginga* when the source was 80 times brighter (Mihara 1995), although the dip around phase 0.45, probably caused by absorption, is shallower.

In order to evaluate the HXD spectra in a model-independent manner, we normalized them to those of the Crab Nebula, acquired in the same detector conditions on 2005

September 15, immediately after the A0535+262 observation. The resulting “Crab ratios”, presented in Figure 2, indicate that the source intensity is ~ 30 mCrab at 20 keV. The ratio keeps rising up to ~ 30 keV, and falls steeply beyond, where the PIN and GSO data both reveal a clear dip feature centered at ~ 50 keV. Since the Crab spectrum is a featureless power-law with a photon index of ~ 2.1 , we may identify this feature with the CRSF of A0535+262 observed previously (§ 1). Although the Crab ratios appear somewhat discrepant between the two HXD components, the effect can be partially explained by different energy resolutions between PIN (~ 3 keV FWHM) and GSO (~ 10 keV FWHM at ~ 50 keV), coupled with the steeply declining spectra. The remainder is within the statistical plus systematic uncertainties.

To quantify the inference from Figure 2, we jointly fitted the PIN and GSO spectra, with the smooth continuum model called NPEX (Negative and Positive power-laws with EXponential; Mihara 1995; Makishima et al. 1999). We left free all but one parameters describing the model; two normalizations, the negative power-law index (α_1), and the exponential cutoff parameter (kT). The positive power-law index, α_2 , was fixed at 2.0, representing a Wien peak, because it was not well constrained by the fit. The interstellar absorption was not incorporated, and the relative PIN vs. GSO normalization was fixed to 1.0 (nominal value). We limited the GSO fitting range to 50–100 keV, because of response uncertainties below 50 keV and the systematic background errors above 100 keV (Fig. 1).

As presented in Figure 3b, the NPEX model was successful with $\chi^2_\nu = 1.23$ ($\nu = 36$) when fitted to the 12–25 keV PIN data and the 73–100 keV GSO data (i.e., excluding the suggested CRSF energy range). When the 50–73 keV GSO data are restored, a worse fit ($\chi^2_\nu = 1.92$, $\nu = 42$) was obtained as shown in Figure 3c. Similarly, inclusion of the 25–70 keV PIN data (but discarding the 50–73 keV GSO data) resulted in a poor fit, with $\chi^2_\nu = 2.13$ for $\nu = 59$ (Figure 3d). The fit became completely unacceptable ($\chi^2_\nu = 2.51$ with $\nu = 65$; Figure 3e) when the entire 12–70 keV PIN data and the 50–100 keV GSO spectra are utilized. Thus, the PIN and GSO data consistently indicate the spectral feature between ~ 25 and ~ 70 keV. This conclusion does not change even considering the systematic background uncertainties (Figure 1).

To better describe the HXD spectra, we multiplied the NPEX continuum with a cyclotron absorption (CYAB) factor (Mihara et al. 1990; Makishima et al. 1999), and repeated the joint fitting. We left free the energy E_a , depth D , and width W of the resonance. As presented in Figures 3a and f, this NPEX×CYAB model is successful in reproducing the PIN (12–70 keV) and the GSO (50–100 keV) spectra simultaneously, with $\chi^2_\nu = 0.89$ for $\nu = 61$. The CYAB parameters were constrained as $E_a = 45.5^{+1.3+0.9}_{-1.3-0.7}$ keV, $D = 1.8^{+0.4+0.5}_{-0.3-0.2}$, and $W = 10.9^{+4.2+2.1}_{-2.9-0.7}$ keV, where the first “ \pm ” represent statistical 90% errors while the

second ones show the effect of systematic background uncertainties. Compared with these, systematic errors in the energy scale determination have smaller effects; the PIN energy scale, reconfirmed by Gd-K lines at 43 keV, is accurate to within 1 keV, and that of GSO, calibrated by several instrumental lines, is reliable to within a few keV. In addition, the systematics in the response matrix are also within statistical errors in the present analysis. The NPEX parameters became $\alpha_1 = -1.62_{-0.31}^{+0.44+0.04}$, and $kT = 12.2_{-0.7-1.3}^{+0.8+0.7}$ keV, with the positive and negative power-law components crossing over at ~ 20 keV (green curves in Fig. 3). This successful NPEX \times CYAB fit reinforces our identification of the feature with the previously known CRSF.

If we instead adopt a “power-law times exponential” continuum with Gaussian absorption (GABS; Kreykenbohm et al. 2004), the HXD data give $E_a = 46.3_{-1.3-1.0}^{+1.5+1.9}$ keV, a Gaussian sigma of $= 4.4_{-0.9-0.3}^{+1.0+0.6}$ keV, and an optical depth of $2.2_{-0.7-0.3}^{+0.9+1.8}$. However, the fit becomes worse; $\chi_\nu^2 = 1.54$ for $\nu = 63$.

Our data are consistent with the presence of the 2nd harmonic feature at ~ 100 keV (see Fig 1), but do not require it, given the current status of the HXD calibration. If the model is multiplied by another CYAB factor with the center energy and width fixed at $2E_a$ and $2W$, respectively, its depth is constrained as $0 \leq D_2 < 1.9$.

4. Discussion

We observed A0535+262 with *Suzaku* in a very low luminosity state, 4.5×10^{35} ergs s^{-1} in 0.5–100 keV, or 3.7×10^{35} ergs s^{-1} in 3–50 keV. In spite of the source faintness (~ 30 mCrab), we successfully detected the CRSF at ~ 45 keV, thanks to the wide energy band and high sensitivity of the HXD. The CRSF was as deep as (or even deeper than) that in the high luminosity states; e.g., $D \sim 0.5$ when the source was two orders of magnitude more luminous (Kendziorra et al. 1994; Grove et al. 1995).

Except for the case of X Persei (Coburn et al. 2001), which exhibits a rather unusual spectrum for an accreting pulsar, the present result provides the detection of a CRSF in the lowest luminosity state ever achieved from a binary X-ray pulsar. Since the CRSF appeared in absorption and not in emission, the Thomson optical depth of the accretion column is inferred to be larger than ~ 10 even with this low luminosity, according to the Nagel model (1981). This conclusion is independently supported by the fact that the pulse profiles (Figure 1) do not differ significantly from those observed in much more luminous outbursts.

In Figure 4, we plot the CRSF energy of A0535+262 versus the 3–50 keV luminosity at

2 kpc, L_x , as measured by *Suzaku* and by previous missions. For consistency with previous works, the *Suzaku* result plotted here is from the GABS modeling. The cyclotron resonance energy of A0535+262 is thus constant within $\pm 10\%$, even though the luminosity changed by nearly two orders of magnitude from 4×10^{35} to 4×10^{37} ergs s⁻¹. Therefore, the implied magnetic field strength, 4.0×10^{12} Gauss, is considered to represent a value intrinsic to this object, which is most likely that on the neutron star surface.

Figure 4 also presents results on the other two pulsars, 4U 0115+63 and X0331+53, mentioned in § 1. The three objects behave in rather different ways on the L_x vs. E_a plane. While 4U 0115+63 and X0331+53 both exhibit luminosity-dependent changes in E_a , the threshold luminosity at which the resonance energy starts changing is significantly different. In addition, A0535+262 does not show such behavior at least up to $\sim 4 \times 10^{37}$ erg s⁻¹.

Considering that accreting X-ray pulsars should form a family described by a rather small number of parameters, one possibility suggested by Figure 4 is that the L_x vs. E_a relation depends systematically on some of the parameters, e.g., the surface field strength itself. Comparing 4U 0115+63 and X0331+53, we may speculate that E_a starts changing at a higher luminosity if the object has a higher surface magnetic field. If this is correct, we would expect the resonance energy of A0535+262 to change at luminosities much higher than so far sampled, because it has the highest magnetic field among known CRSF pulsars.

Alternatively, the values of L_x in Figure 4 may be subject to systematic errors, due, e.g., to uncertainties in the source distance, and/or to the anisotropy of emission that is inherent to X-ray pulsars. (The luminosities are all calculated assuming isotropic emission.) If the luminosity is corrected for these factors, the behavior of E_a in Figure 4 might become essentially the same among the three objects.

To distinguish between these two possibilities (or to arrive at yet another alternative), we need further observations. In either case, it must be examined whether the variable column-height scenario, which was successful on 4U 0115+63 (Mihara et al. 1998, 2004; Nakajima et al. 2006), can be applied also to A0535+262 and X0331+53.

The authors would like to thank all the members of the *Suzaku* Science Working Group, for their contributions in the instrument preparation, spacecraft operation, software development, and in-orbit instrumental calibration.

REFERENCES

Arnaud, K.A., 1996, in Astron. Data Analysis Soft. and System V. ASP Conf. Ser., 101, 17

- Boldt, E 1987 IAUS..124..611B
- Coburn, W, Heindl, W.A, Gruber, D.E. et al. 2001 ApJ, 552, 738
- Grove, J.E., Strickman, M.S., Johnson, et al. 1995, ApJ, 438, L25
- Inoue, H., Kunieda, H., White, N., et al. 2005, Astron. Telegram #613
- Kawaharada, M., Hong, S. et al. 2004, SPIE, 5501, 286
- Kendziorra, E., Kretschmar, P. et al. 1994, A&A, 291, L31
- Kokubun, M. et al. 2006, PASJ in preparation
- Kretschmar, P., Kreykenbohm, I. et al. 2005, Astron. Telegram #601
- Kreykenbohm, I., Wilms, J., Coburn, W., et al. 2004, A&A, 427 975
- Makishima, K., Mihara, T., Nagase, F. & Tanaka, Y. 1999, ApJ, 525, 97
- Matsumoto, H., Koyama, K., Tsuru, T.G. et al. 2005, NIM A, 541, 357
- Mihara, T., Makishima, K., Ohashi, T., Sakao, T. & Tashiro, M. 1990, Nature 346, 250
- Mihara, T., Ph.D. thesis in Univ. of Tokyo 1995
- Mihara, T., Makishima, K., & Nagase, F. 1998, Adv. Space Res. 22, 987
- Mihara, T., Makishima, K., & Nagase, F. 2004, ApJ, 610, 390
- Mowlavi, N., Kreykenbohm, I., Shaw, et al. 2006, A&A, in print.
- Nagel, W., 1981, ApJ, 251, 288
- Nakajima, M., Mihara, T., Makishima, K., & H. Niko, 2006, ApJ 646, 1125
- Nakajima, M., Ph.D. thesis in Nihon Univ. 2006b
- Negueruela, I., & Okazaki, A. T., 2001, A&A, 369, 108
- Negueruela, I., Roche, P., Fabregat, J., & Coe, M. J. 1999, MNRAS, 307, 695
- Steele, I. A., Negueruela, I., Coe, M.J., & Roche, P. 1998, MNRAS, 297, L5
- Wilson, C. A., & Finger, M.H. 2005, Astron. Telegram #605

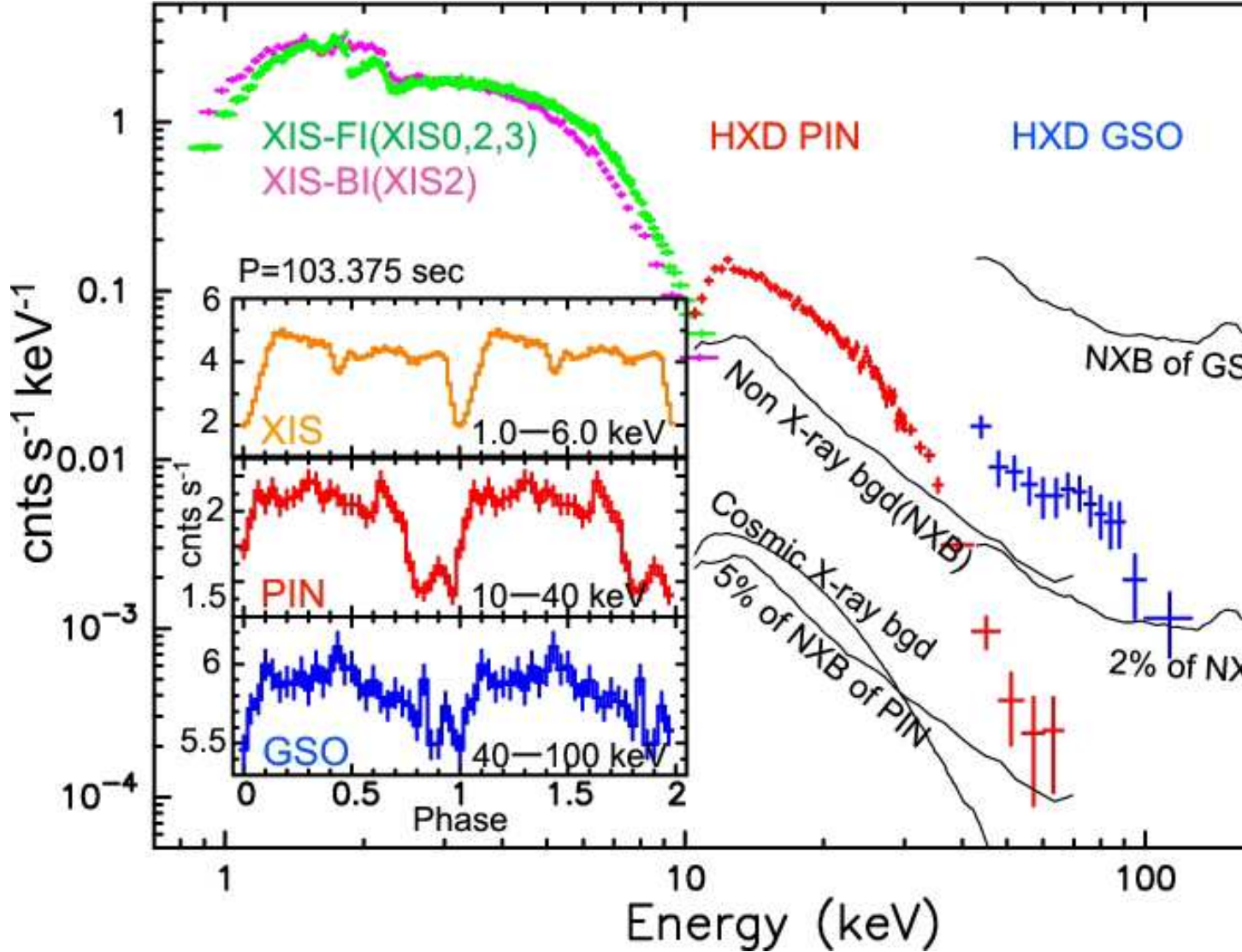


Fig. 1.— Time-averaged and background-subtracted spectra of A0535+262, obtained with the *Suzaku* XIS (green and purple) and HXD (red and blue). They are presented without removing instrumental responses, and error bars are statistical only. Non X-ray backgrounds of PIN and GSO, their uncertainties (see text), and the estimated cosmic X-ray background (Boldt 1987) are shown in solid lines. The inset shows background-inclusive pulse profiles in three typical energy bands, obtained by folding the data at the pulsation period. The relative timings between XIS and HXD are not calibrated yet.

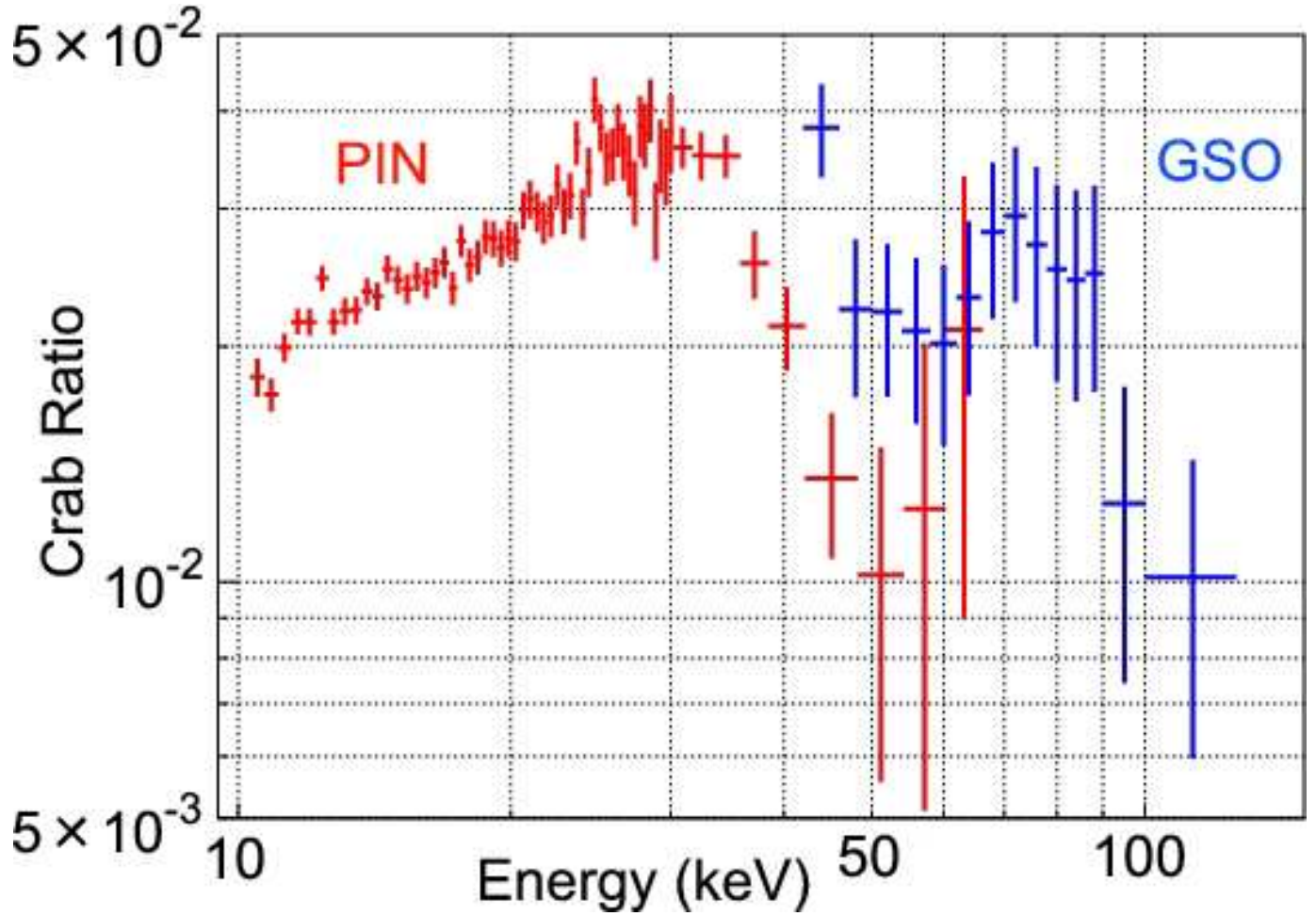


Fig. 2.— Ratios of the background-subtracted HXD spectra of A0535+262 to those of the Crab Nebula. The data obtained with the HXD PIN and GSO are shown in red and blue, respectively. Error bars are statistical only.

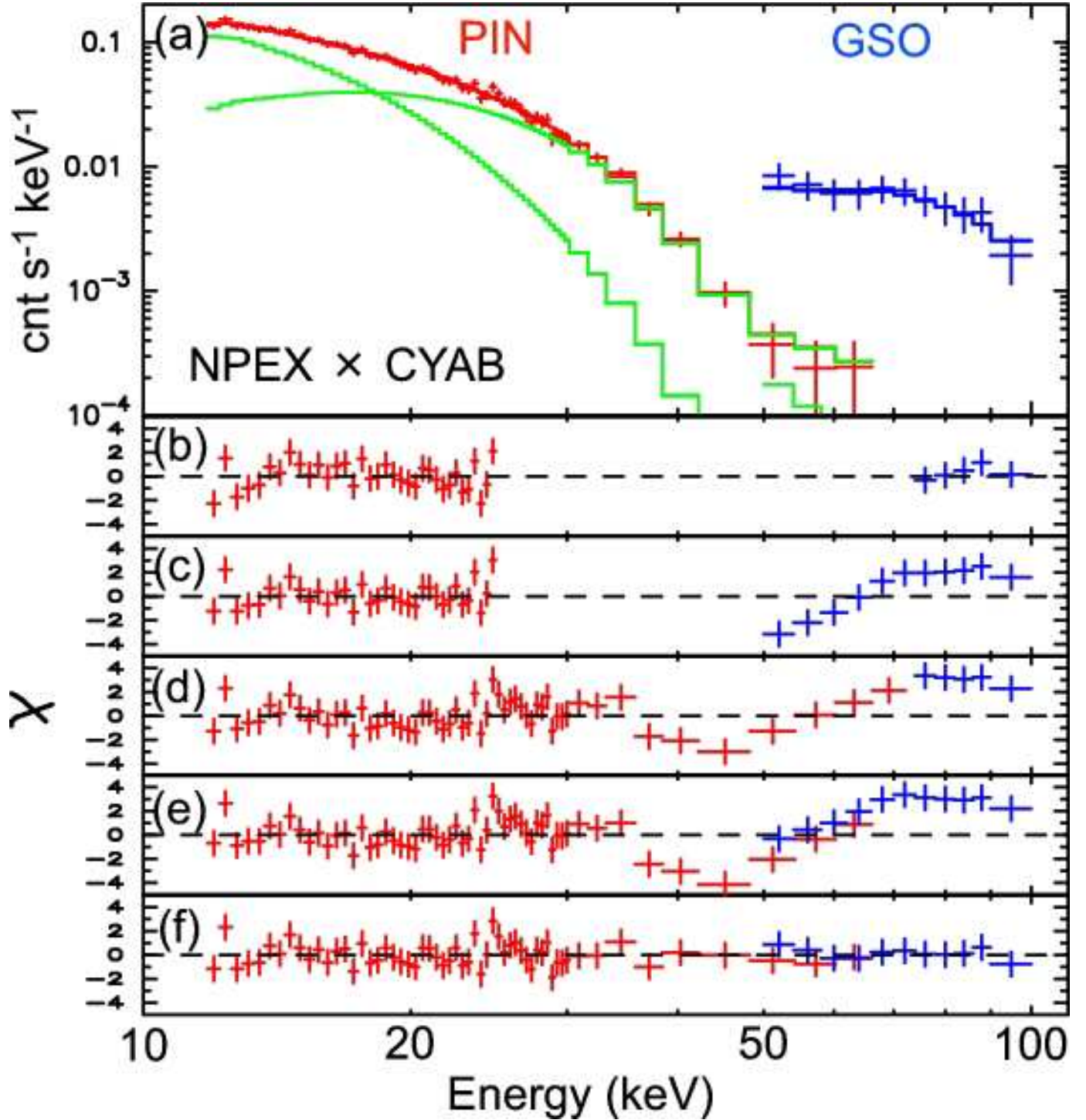


Fig. 3.— Model fittings to the pulse phase-averaged HXD spectra of A0535+262. Panel (a) shows the NPEX × CYAB fit in comparison with the data, and panel (f) the data-to-model ratio. In panels (b) through (e), the PIN and GSO data are divided by the best-fit NPEX models (without incorporating the CYAB factor) obtained using different energy ranges (see text).

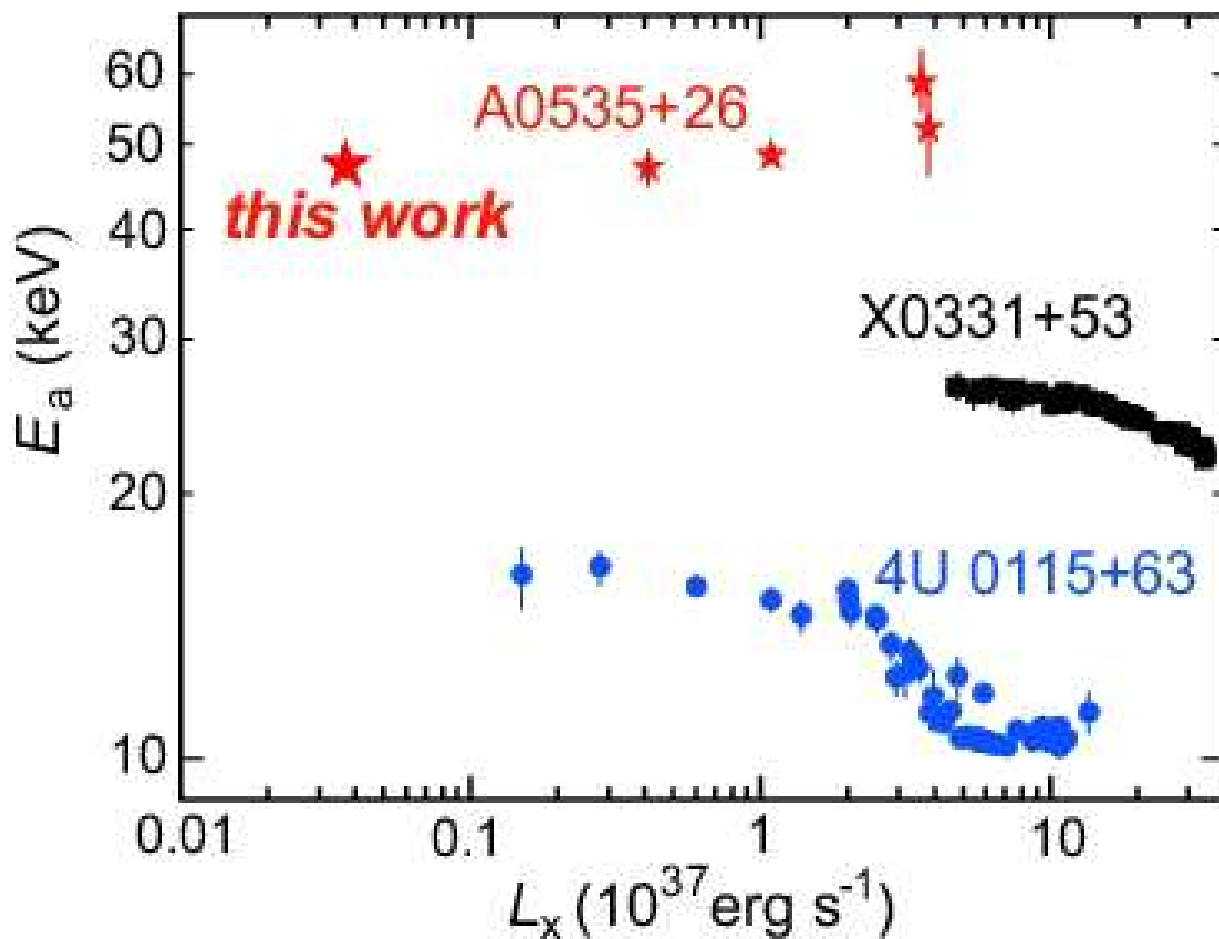


Fig. 4.— Luminosity (3–50 keV) dependence of the fundamental cyclotron resonance energies in binary X-ray pulsars, using Gaussian absorption modeling. The other data points for A0535+262 refer to Wilson & Finger (2005; $L_x = 1.1 \times 10^{37} \text{ ergs s}^{-1}$), Kretschmar et al. (2005; 0.4×10^{37}), Grove et al. (1995; 3.6×10^{37} , assuming 110 keV as the 2nd harmonic), and Kendziorra et al. (1994; 3.8×10^{37}). The results on 4U 0115+63 and X0331+53, both assuming a distance of 7 kpc, are from Nakajima et al. (2006) and Nakajima (2006b), respectively.